

Onboard implementation of the GHER model for the Black Sea, with SST and CTD data assimilation

L Vandembulcke, A Capet, J M Beckers, M Grégoire & S Besiktepe

To cite this article: L Vandembulcke, A Capet, J M Beckers, M Grégoire & S Besiktepe (2010) Onboard implementation of the GHER model for the Black Sea, with SST and CTD data assimilation, Journal of Operational Oceanography, 3:2, 47-54, DOI: [10.1080/1755876X.2010.11020117](https://doi.org/10.1080/1755876X.2010.11020117)

To link to this article: <https://doi.org/10.1080/1755876X.2010.11020117>



Published online: 01 Dec 2014.



Submit your article to this journal [↗](#)



Article views: 163



View related articles [↗](#)



Citing articles: 2 View citing articles [↗](#)

Onboard implementation of the GHER model for the Black Sea, with SST and CTD data assimilation

*L Vandembulcke, A Capet, J-M Beckers and M Grégoire, GeoHydrodynamics and Environment Research, Université de Liège, Belgium
S Besiktepe, NATO Undersea Research Centre, La Spezia, Italy*

The first operational implementation of the GHER hydrodynamic model is described. It took place onboard the research vessel *Alliance* with all computation and sharing of forecasts being realised from the vessel in near-real time. The forecasts were realised in the context of the Turkish Straits System 2008 campaign, which aimed at the real-time characterisation of the Marmara Sea and (south-western) Black Sea. The model performed badly at first, mainly because of poor initial conditions. Hence, as the model includes a reduced-rank extended Kalman filter assimilation scheme, after a hindcast where sea surface temperature and temperature and salinity profiles were assimilated, the model yielded realistic forecasts. Furthermore, the time required to run a one-day simulation (about 300 seconds of simulation, or 500 with pre-processing and data transfers included) was very limited and thus operational use of the model is possible.

INTRODUCTION

The ‘Turkish Straits Systems 08’ (TSS08) cruise took place in September 2008 with the aim of a process-oriented real-time characterisation of a marine region, in this case the Dardanelles Strait, the Marmara Sea and the Western Black Sea. During the campaign, numerous *in-situ* measurements were carried out onboard the research vessel R/V *Alliance* as well as some other small ships of the riparian countries. Processes of different scales were measured: large scale hydrographic surveys provided a synoptic view of the basin, but mesoscale and sub-mesoscale measurements were also carried out by means of towed yoyo-systems, CTD chains, gliders, etc. Fixed moorings also provided measurements of currents, sea level, temperature and salinity.

Furthermore, satellite observations were acquired and sent in near real-time to the research vessel and different ocean circulation models were also run onboard. In particular, the HOPS^{1,2} and GHER³ models were used.

The present study focuses on the near real-time implementation of the GHER model in the Black Sea with a 5km

horizontal resolution. The authors examine whether the model can be run fast enough for delivering timely forecasts of reasonable skill, and what requirements are needed. The model domain was pre-implemented on a bootable external USB hard drive, which was brought onboard the vessel on 19 September 2008; simulations were only carried out from that day on. Some hindcasts had started on 16 August and were run up to 15 September, and compared with measurements. Afterward, the model was run up to 19 September, and then daily in order to provide operational forecasts, up to the end of September.

This paper also describes the GHER hydrodynamic model and its data assimilation scheme, and then examines the model results during the cruise.

GHER MODEL AND DATA ASSIMILATION SCHEME

The GHER hydrodynamic model (available online^(a) with a user-manual^(b)) is a free-surface primitive equation model developed in the early 1990s. It forecasts the prognostic

variables of temperature, salinity, sea surface elevation, horizontal velocity and turbulent kinetic energy, using the hydrostatic, β -plane and Boussinesq approximations. Horizontally, it uses an Arakawa-C grid. In the vertical, it uses a double sigma coordinate, ie, the domain is split in two parts in the vertical, the limit being at 170m depth. In each part, a sigma coordinate is used. The model integration scheme is conservative for tracers. Furthermore, the model uses mode splitting: for computational efficiency, the baroclinic timestep is much larger than the barotropic one. The vertical turbulence parameterisation uses a k turbulent kinetic energy closure scheme described in Nihoul *et al.*⁴ Further information about the model can be found in Beckers³ and, with the GHER model having already been implemented in various basins, details about its implementation in the Black Sea with horizontal resolutions of 15 and 5 km.⁵

The GHER model code is written to be run on parallel computers, with OpenMP or with PVM. It comprises a data assimilation procedure described below, a nesting procedure for rapid-relocatable nested grids,⁶ and a module to couple it with passive tracers, eg, for ecosystem models.⁷ The latter two possibilities are not used in the present implementation.

The model is accompanied by the Singular Evolutive Extended Kalman (SEEK) data assimilation (DA) filter.^{8,9} This DA scheme is a reduced-rank approximation of the Extended Kalman filter. In the latter filter, only the first- and second-order moments of the error statistics are retained. Thus, it is supposed that the anomalies can be considered quasi-linear, and the model error is approximately Gaussian. This is obviously not the case, but, for relatively short time forecasts, the authors will still use this widespread approach. The low-rank model error covariance matrix is built based upon empirical orthogonal functions (EOFs) representing the model error variability.

The implementation allows to use full 3-D multivariate (temperature (T), salinity (S) and sea surface elevation (η) EOFs. Hence, whenever data is assimilated, this leads to corrections on the T , S , and η variables. These corrections are then localised in space:¹⁰ they are multiplied by a radial Gaussian function centred on the corresponding observation in order to limit the spatial extent of the correction that an observation can yield. In the present case, the Gaussian's extent is put to 100km. Note that if the model error covariance matrix would accurately represent the model error covariance, this step would not be necessary; unphysical long-range correlations would not be present in the computed statistics. Finally, in view of the large scales of interest, the geostrophic velocity correction (corresponding to the T , S and η corrections) is computed and applied to the model horizontal velocity variables U and V .

Some specific aspects of the current implementation are given hereafter. Although the region of interest is the South-Western Black Sea, the authors' model domain covers the

whole basin in order to avoid (unknown) open sea boundary conditions. The model bathymetry is the Smith and Sandwell¹¹ bathymetry with smoothing. The horizontal resolution is 0.045 deg, corresponding to 4km and 5km for longitude and latitude respectively; this is smaller than the first internal radius of deformation which is 20km in the Black Sea.¹² The model uses 31 vertical levels. The barotropic and baroclinic timesteps are 15s and 900s respectively.

With these settings, the model (using OpenMP parallelisation) takes about 5 min to simulate one day on a modern computer with an Intel quad-core CPU. Note that another implementation with a horizontal resolution of about 2km, and timesteps of 2.5s and 150s respectively, requires about 2.5h for one day of simulation; it was not used operationally during this experiment.

The sea-atmosphere fluxes are computed interactively with bulk formula; the atmospheric forcing fields forecasts (for air temperature, air dew temperature, wind speed and atmospheric pressure) are obtained in near real-time from the COAMPS model.

The cloud coverage field was unavailable and obtained from the NCEP forecasts website. Finally, the Bosphorus and six rivers (Danube, Dnestr, Dniepr, Kisil-Irmak, Rioni, and Sakarya) are represented in the model with imposed fluxes obtained from hydrological simulations for the year 2000.¹³ It was decided to start the model on 16 August, two weeks before the actual TSS08 start, and a few days after the start of COAMPS forcing fields availability. Initial conditions were taken from the MODB/MEDAR4 monthly climatology.¹⁴ Data from the HYDROBLACK91 campaign¹⁵ could also have served to build an initial condition, but this was not more recent than the climatology and did not correspond particularly to the condition of the month August.

RESULTS

Hindcast with data assimilation

Output fields from the simulation starting on 16 August and ending on 15 September were compared with sea surface temperature (SST) images obtained during the cruise from the MODIS satellite^(c); it could immediately be seen that the forecast was not adequate (the root mean square error between model forecast and the first SST image was 2.32°C, see Table 1). The inadequacy was attributed mainly to an inappropriate initial condition, obtained from a climatology over 15 years old.

Thus, it was decided to restart this simulation while assimilating both SST images and temperature and salinity profiles obtained from CTD measurements onboard the research vessel. It was hoped that the joint assimilation of synoptic surface data and vertical profiles would consistently correct the 3-D field. However, the data assimilation scheme requires an estimation of the model error covariance matrix,

| | 1 | 2 | 3 | 4 | 5 | 6 | 7 | 8 |
|--------------------|------|------|------|------|------|------|------|------|
| Date | 24/8 | 25/8 | 27/8 | 29/8 | 4/9 | 5/9 | 6/9 | 9/9 |
| Forecast rms error | 2.32 | 1.54 | 1.07 | 1.43 | 2.23 | 1.65 | 1.86 | 1.55 |
| Analysis rms error | 0.71 | 0.83 | 0.59 | 1.11 | 1.36 | 1.22 | 1.28 | 1.08 |

Table 1: Root mean square difference between SST observations and model forecast and analysis [°C]

which was not available. Therefore, it was decided to use the (time) variability of the model during the previous hindcast as a proxy for the error covariance. Fifteen multi-variate EOFs were thus obtained; each variable (T , S , η) was normalised according to the variable's variance and the corresponding grid cell size.

It was noted from the start that this relatively small rank (15) would probably not allow mesoscale corrections. Another approximation in the data assimilation procedure consisted of not updating the model error space but rather keeping these 15 EOFs constant in time. The observations error covariance matrix was chosen diagonal, with standard deviations of 1°C and 0.7 psu for the CTD measurements of temperature and salinity respectively, and 50°C for the MODIS SST data. Although the latter standard deviation might look pretty large, it is chosen to account for the representativity error due to the high spatial resolution of the SST observations (with respect to the spatial resolution of CTD measurements and of the model).

Eight SST maps were selected between 24 August and 9 September (each of them around 11:00 in the morning); the other available images were affected by many clouds. There were 182 CTD profiles between between 26 August and 11 September, but some of them were in the Straits (South-West of the actual Black Sea): CTD profiles in the Black Sea were only available between 2 and 8 September. However, the data assimilation scheme allows out-of-grid observations to be included, and discards them automatically. Thus, no preprocessing was applied to the CTD data, and all of them were simply listed in chronological order in the model's data assimilation parameters file. Finally, note that only the western half of the Black Sea was covered by the CTD measurements and the (available part of the) SST images; hence no direct corrections were applied to the eastern part.

Table 1 shows the root mean square (rms) difference between SST observations and the model forecast (ie, independent data, just before assimilation) and model analysis (just after assimilation). It can be seen that the mean difference before the first assimilation cycle, on 24 August, is large (2.32°C), but strongly reduced with DA. Then, in between SST assimilation cycles, the model slightly increases the rms error.

After the third SST analysis, CTD profiles are also assimilated. The rms differences between the model forecast and CTD profiles are shown in Fig 1. Concerning temperature, the average error between measurements and model forecast is 1.58°C; data assimilation reduces this to 0.69°C. The error on forecasted salinity is 0.35 psu, reduced to 0.33 psu by data assimilation.

The strongly approximated model error covariance matrix might create instabilities or at least inconsistent updates. Hence, between the fourth and the seventh SST assimilation cycles, the model (and CTD assimilation cycles) relatively strongly increases the surface temperature rms error; but of course SST assimilation cycles in turn reduce that rms error. It can be supposed that a part of the error remaining after the latest DA cycles (1.3 to about 1.1°C, relative to SST images, see Table 1) is due to this back-and-forth game of corrections due to SST and CTD observations. The remaining part is orthogonal to the (low rank) model error space, and could never be corrected with our setup.

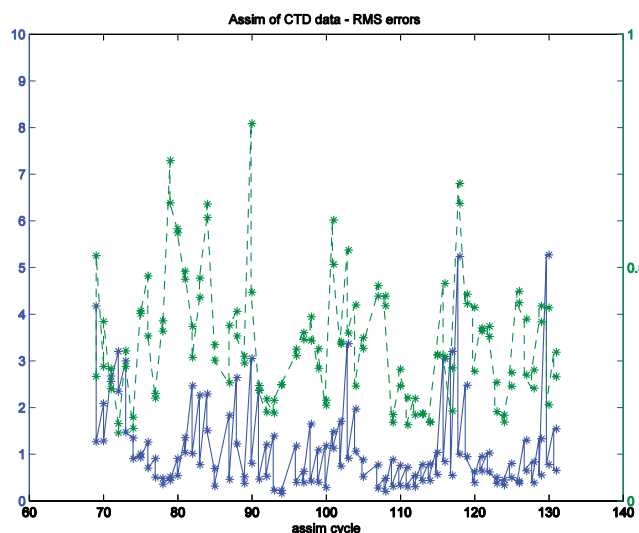


Fig 1: Temperature (full line, blue) and salinity (dashed line, green) rms error before and after each assimilation of CTD profiles

Figs 2 to 5 show the effect of data assimilation on model surface temperature. As announced before, assimilation of the first SST image (covering from about 30°E to 35°E) strongly heats the whole western basin, by 1.5°C up to 4°C (Fig 3). However, the realistic cold water mass along the western part (around 42°N, 33°E) of the southern coast is also heated away (Fig 2). This cold water will be re-created by the model and by later assimilation cycles, particularly the SST assimilated on 6 September (see Fig 4). Of course, the eastern part of the basin (and in the case of the first assimilation cycle, the western coast not covered by data) are not corrected.

From the second SST assimilation cycle on, the effect of assimilation is still mostly heating, but not everywhere anymore: some parts of the domain are cooled. The heating trend during assimilation cycles may be caused by too cool water still flowing in the western half basin from the uncorrected eastern half basin. However, corrections tend to become smaller and smaller. Fig 5 shows the effect of assimilation of a temperature and salinity profile; the 100th CTD profile is chosen as an example. The effect is mainly to put back in place the cold water mass along the Turkish coast.

Finally, the model fields were also compared to independent (not assimilated) measurements obtained by a scanfish[®] towed by the *Alliance* between 3 and 6 September 2008. At that time, the ship was in the region ~41°N,

| | Temp, no DA | Temp, DA | Salinity, no DA | Salinity, DA |
|-------------------------|----------------|-------------|--------------------|-----------------|
| Bias | 0.81°C | -0.61°C | 0.209 psu | 0.05 psu |
| Unbiased rms | 4.07°C | 2.7°C | 0.196 psu | 0.374 psu |
| Correlation | 0.81 | 0.92 | 0.87 | 0.87 |

Table 2: Root mean square difference between independent scanfish observations, for the hindcast without (cols 1 and 3) and with (cols 2 and 4) data assimilation, for temperature [°C] and salinity [psu]

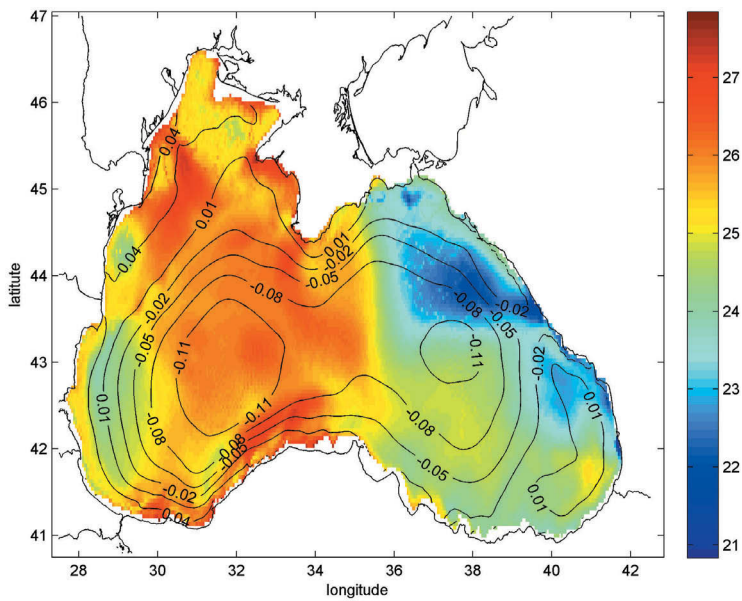
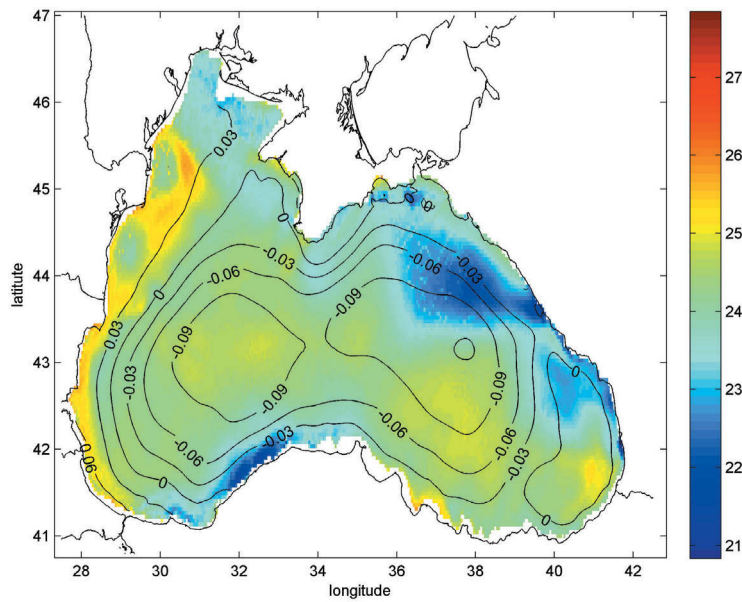


Fig 2: Surface temperature [°C] and elevation [m] of the forecast on 24 August at 10:15, before (top panel) and after (bottom panel) assimilation of SST data in the western half of the basin

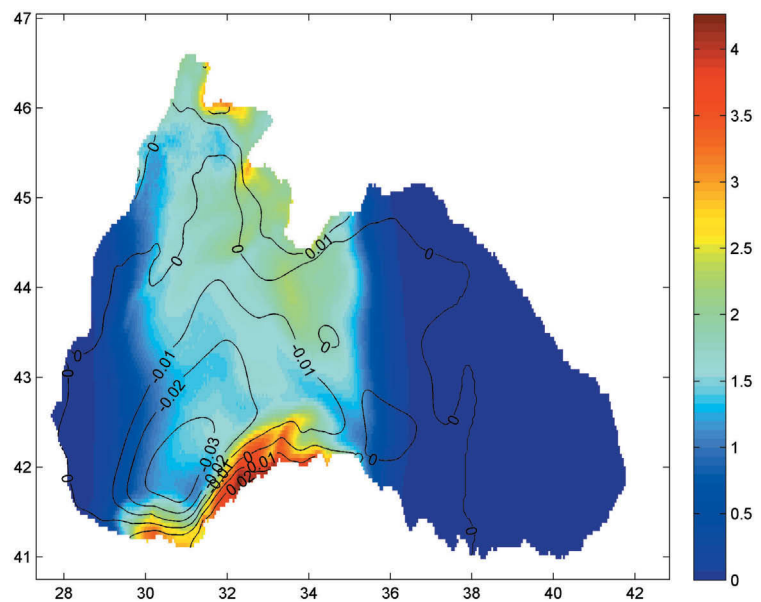


Fig 3: Modification of SST data assimilation on the surface temperature [°C] and elevation [m] on 24 August 10:15. (This figure equals Fig 1 bottom minus top)

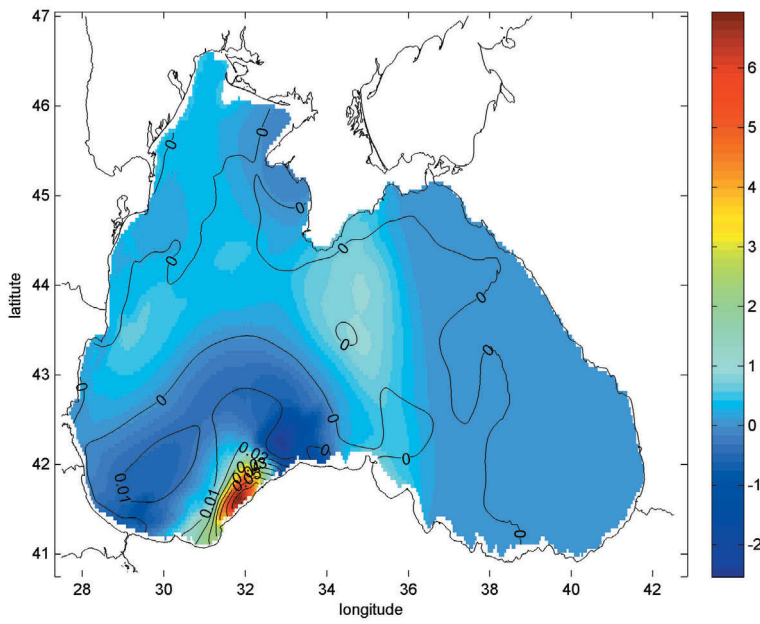


Fig 4: Modification of SST data assimilation on the surface temperature [°C] and elevation [m] on 6 September 10:25

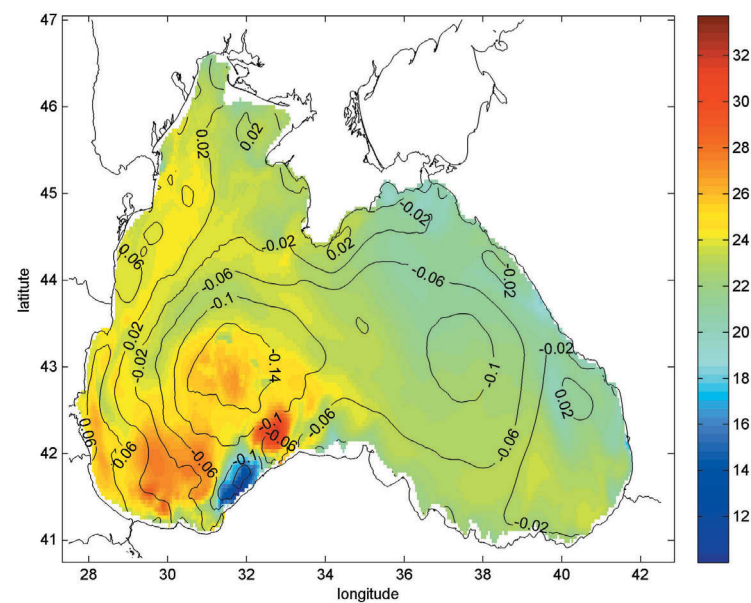
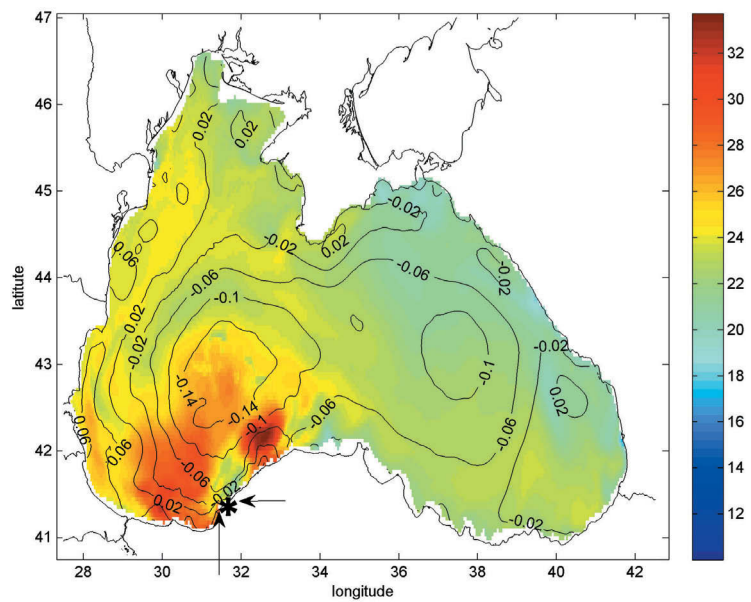


Fig 5: Surface temperature [°C] and elevation [m] of the forecast on 5 September at 21:58, before (top panel) and after (bottom panel) assimilation of CTD data. The CTD location (around 41.5°N, 31.5°E) is indicated with a star (see arrows) in the upper panel

28–30°E, close to the Bosphorus mouth. Earlier measurements were obtained while the vessel was in the Bosphorus Straits, which is parameterised but not modelled. Results from the comparison are shown in Table 2. It can be seen that assimilation of CTD and satellite SST data reduces bias towards the scanfish data by 25% (temperature) and 75% (salinity). On average, the model which was too warm without data assimilation, becomes rather too cold, at least at the locations of the scanfish data.

The unbiased rms error is strongly reduced for the temperature, but increases for salinity. The linear correlation is also improved for temperature, and unmodified for salinity.

Operational forecasts

The hindcast simulation described was continued daily, in forecasting mode, starting on 20 September. Operational forecasts were run every day as soon as the COAMPS

atmospheric forcing fields were available. The model currently requires atmospheric forcing fields in its own binary format; the conversion takes just a couple of seconds with the proper scripts. Afterward, the simulation takes about 5 min for one day of forecast. Outputs are written directly in netCDF format¹⁶ which were then stored on the cruise's database.

Generally speaking, the forecasts showed good agreement with the data (MODIS SST mages and *in-situ* measurements). Comparison with HOPS, the other model run onboard the *Alliance*, was difficult due to differences between the two setups. In particular, the HOPS model was implemented on a domain covering only the south-western part of the Black Sea, hence using open sea boundary conditions. Nevertheless, Figs 6 and 7 show the SST forecasts of the GHER and HOPS models, and the closest (in time) MODIS image. With respect to this SST image, the GHER model forecast is good, except

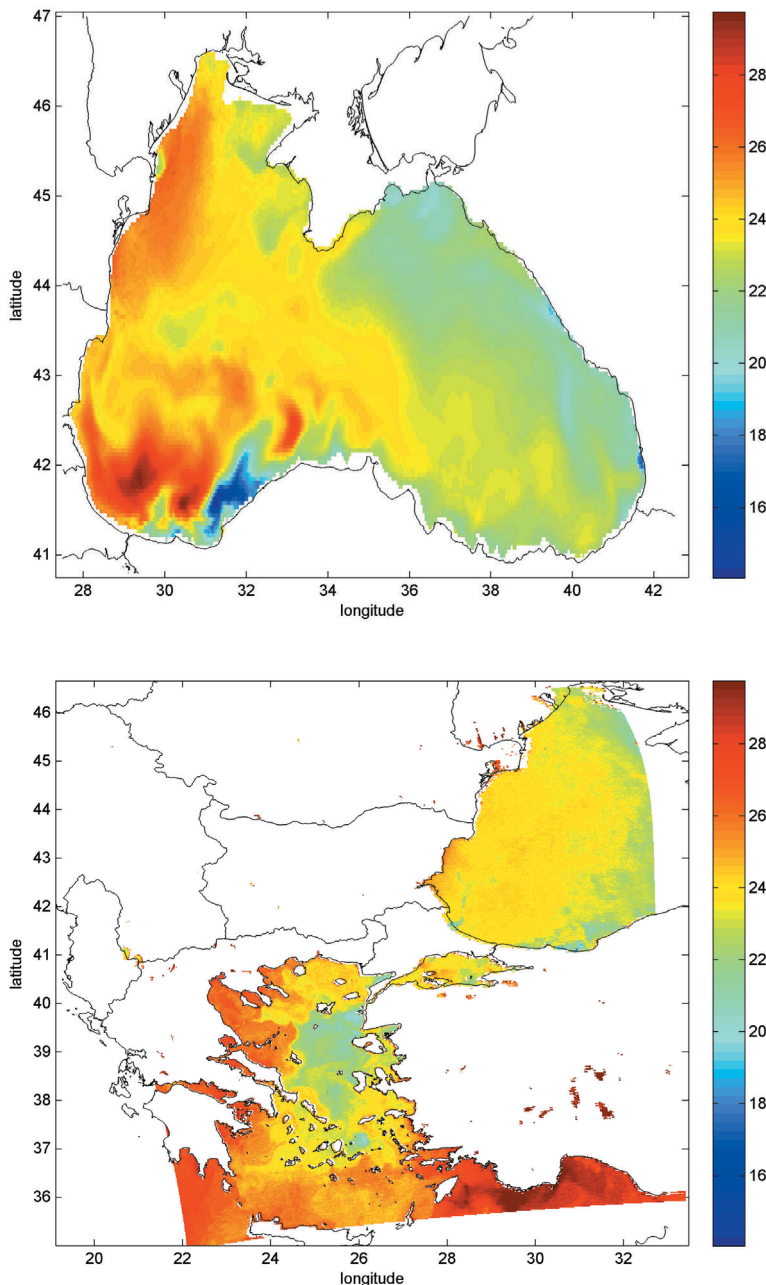


Fig 6: Forecast of SST by the GHER model on 8 September; midday (top panel), and MODIS SST on 8 September, 10:55 (bottom panel)

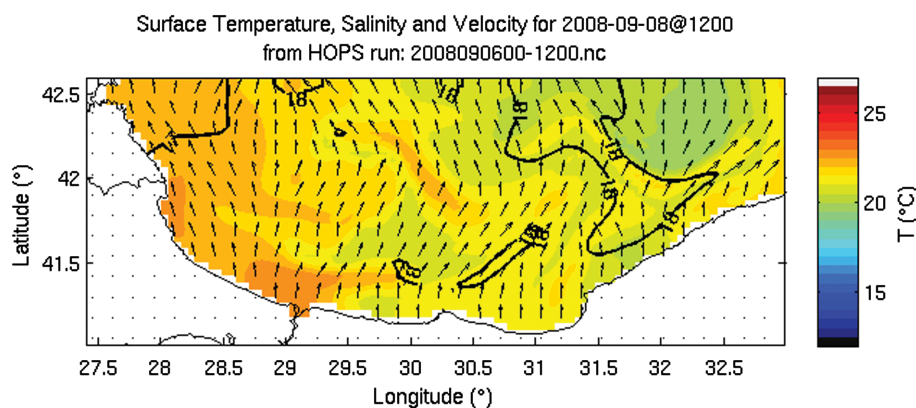


Fig 7: Forecast of SST by the HOPS model on 6 September, midday

the cold water area along the Turkish coast which is really too cold (too strong correction during the latest assimilation cycle). The HOPS model forecast looks generally too cold by 2° or 3°C, but the cold area along the Turkish coast is not over-cooled like in the GHER model; it is rather too warm in the HOPS model.

CONCLUSIONS

In this article the authors have explained an operational implementation of the GHER model in the Black Sea during the TSS08 campaign. The model code was pre-configured and stored on a bootable external USB hard drive. The drive was connected on a computer with an Intel quad-core CPU. First, a month of hindcast simulations was carried out. Mostly because of relatively bad initial conditions coming from a 15-year old climatology, the model forecasts were bad (compared to SST images). Hence, the hindcast was started over, and this time eight SST images and about 100 CTD temperature and salinity profiles were assimilated. The effect of data assimilation was very large and resulted in a strong heating of the model temperature during the first assimilation cycles (1.6°C during the first cycle); but the following cycles lead to more modest and local effects.

Following the hindcast simulations, daily operational forecasts were carried out up to the end of September, with resulted in good agreement with observations. On a modern personal computer (with a CPU with 4 cores), one day of simulation required about 300 seconds, plus a few minutes to download and convert the atmospheric forcing fields into the desired format. Outputs were saved directly to netCDF format by the model, and stored on the campaign database.

REFERENCES

- (a) <http://modb.oce.ulg.ac.be/viewsvn/>
- (b) <http://modb.oce.ulg.ac.be/mediawiki/index.php/Category:GHER3D>
- (c) <http://modis.gsfc.nasa.gov>
- (d) <http://www.eiva.dk/sw298.asp>
1. Robins AR, Arango HG, Warn-Varnas A, Leslie WG, Miller AJ, Halcy PJ and Lozano CJ. 1996. *Real-time regional forecasting*. Modern approaches to data assimilation in ocean modelling. Elsevier.
2. Lozano CJ, Robinson AR, Arango HG, Gangopadhyay A, Sloan NQ, Haley PJ and Leslie WG. 1996. *An interdisciplinary ocean prediction system: Assimilation strategies and structured data models*. Modern approaches to data assimilation in ocean modelling, pp413–452. Elsevier
3. Beckers J-M. 1991. *Application of a 3D model to the Western Mediterranean*, Journal of Marine Systems, 1, 315–332.
4. Nihoul JCJ, Deleersnijder E and Djenidi S. 1989. *Modelling the general circulation of shelf seas by 3D $k - \epsilon$ models*. Earth Science Reviews, 26, 163–189.
5. Beckers J-M, Gregoire M, Nihoul JCJ, Stanev E, Staneva J and Lancelot C. 2002. *Modelling the Danube-influenced north-western continental shelf of the Black Sea*. In: *Hydrodynamical processes simulated by 3D and box models*. Estuarine, Coastal and Shelf Science, 54, 453–472, doi:10.1006/ecss.2000.0658.
6. Barth A, Alvera-Azcarate A, Rixen M and Beckers J-M. 2005. *Two-way nested model of mesoscale circulation features in the Ligurian Sea*. Progress in Oceanography, 66, 171–189, doi:10.1016/j.pocean.2004.07.017.
7. Grégoire M and Beckers, J. M. 2004. *Modelling the nitrogen fluxes in the Black Sea using a 3D coupled hydrodynamical-biogeochemical model: transport versus biogeochemical processes, exchanges across the shelf break and comparison of the shelf and deep sea ecodynamics*. Biogeosciences, 1, 33–61.
8. Pham DT, Verron J and Roubaud MC. 1998. *A singular evolutive extended Kalman filter for data assimilation in oceanography*. Journal of Marine Systems, 16, 323–340.
9. Brasseur P, Ballabrera J and Verron J. 1994. *Assimilation of altimetric data in the mid-latitude oceans using the Singular Evolutive Extended Kalman filter with an eddy-resolving, primitive equation model*. Journal of Marine Systems, 22, 269–294.
10. Testut CE, Brasseur P, Brankart J-M and Verron J. 2003. *Assimilation of sea-surface temperature and altimetric observations during 1992–1993 into an eddy permitting primitive equation model of the North Atlantic Ocean*. Journal of Marine Systems, 40, 291–316.
11. Smith WHF and Sandwell DT. Global sea floor topography from satellite altimetry and ship depth soundings, Science, 277, 1956–1962.
12. Ozsoy E and Unluata U. 1997. *Oceanography of the Black Sea: A review of some recent results*. Earth Science Reviews, 42(4), 231–272.

13. Ludwig W, Dumont E, Meybeck W and Heussner S. 2009. *River discharges of water and nutrients to the Mediterranean and Black Sea: Major drivers for ecosystem changes during past and future decades*. Process in Oceanography, in press.
 14. Brasseur P, Beckers J-M, Brankart JM and Schoenauen R. 1996. *Seasonal temperature and salinity fields in the Mediterranean Sea: Climatological analyses of an historical data set*. Deep Sea Research, 43, 159–192.
 15. Aubrey DG, Oguz T, Demirev E, Ivanov V, McSherry T, Diaconu V and Nikolaenko E. 1992. Hydroblack '91 CTD Intercalibration Workshop. In: IOC Workshop Report No 91.
 16. Russel K, Rew R, Hartnett EJ and Caron J. 2006. *NetCDF-4: Software implementing an enhanced data model for the geosciences*. In: 22nd International conference on interactive information processing systems for meteorology, oceanography, and hydrology, American Meteorological Society.
-